Slides for a
Lecture at Princeton University
by Frank H. Stillinger
Chemical Engineering Department
December 1, 2000

Weird Science:
The Gaussian Core Model

Weird Science: The Gaussian Core Model. Outline

Reference: *Principles of Polymer Chemistry* by Paul J. Flory

Integration of the interaction free energy for a pair of molecules

Two self-avoiding polymers

Polymer center of mass potentials

Gaussian core model basic pair interactions

Rigid sphere limit

T=0 duality relation

Temperature vs. density

Phase diagram of the GCM

Pressure vs. temperature from the molecular dynamics simulation

Pressure vs. temperature—fluid phase

Temperature vs. density

Low-order irreducible clusters

High-temperature series coefficients for the Gaussian core model excess free energy

(contents continued on next page)

Home

Slides for a
Lecture at Princeton University
by Frank H. Stillinger
Chemical Engineering Department
December 1, 2000

Weird Science:
The Gaussian Core Model

Eighth-order cluster contributions

Eighth-order cluster contributions

Compression and Gaussian smoothing

Collective coordinate representation

Structure factor S(Q)

Coexistence parameters for T=0 structural transition

Challenges to synthetic chemistry and to theoretical modeling

Home

Weird Science: The Gaussian Core Model

- Historical background: Polymer chemistry
- Mathematical model
- Hard-sphere limit
- Lattice energy duality $(T = 0)$
- Phase diagram
- Simulation results
- Expansions in $\beta = (k_B T)^{-1}$
- Compression and Gaussian smoothing
- $T > 0$ duality
- Research challenges

Collaborators: T.A. Weber, D.K. Stillinger

PRINCIPLES OF POLYMER CHEMISTRY

By Paul J. Flory

Professor of Chemistry, Cornell University

Cornell University Press

ITHACA, NEW YORK, 1953

termination of the fundamental thermodynamic parameters from osmotic or light-scattering measurements is an unfortunately difficult matter owing to the secondary dependence of the observed thermodynamic behavior on the molecular configuration.

APPENDIX

Integration of the Interaction Free Energy for a Pair of Molecules.[24] —We require, according to Eq. (53), the integral $\int \rho_k \rho_l \delta V$ over the total volume, when the centers of the polymer molecules k and l are separated by the distance a; ρ_k and ρ_l, the segment density distributions for the respective molecules about their centers, are assumed to be given with sufficient accuracy by Gaussian distributions (Eq. 51). Since the chain lengths of the molecules are taken to be identical, the Gaussian parameters β' characterizing their distributions will be identical. It is convenient to choose cylindrical coordinates, r^* and θ with origin midway between the molecules. Then

$$\begin{aligned} s_k^2 &= a^2/4 + ar^* \cos\theta + r^{*2} \\ s_l^2 &= a^2/4 - ar^* \cos\theta + r^{*2} \end{aligned} \tag{A-1}$$

Substituting these relations in the Gaussian expression, Eq. (51), for ρ_k and ρ_l, and inserting them in the required integral

$$\begin{aligned} \int \rho_k \rho_l \delta V &= (x^2\beta'^6/\pi^3) \int_0^\infty \int_0^\pi \exp[-\beta'^2(a^2/2 + 2r^{*2})] 2\pi r^{*2} \sin\theta dr^* d\theta \\ &= (4x^2\beta'^6/\pi^2) \exp(-\beta'^2 a^2/2) \int_0^\infty \exp(-2\beta'^2 r^{*2}) r^{*2} dr^* \\ &= [x^2\beta'^3/(2\pi)^{3/2}] \exp(-\beta'^2 a^2/2) \end{aligned} \tag{A-2}$$

Substituting this result in Eq. (53), we have for the free energy change associated with the transfer of molecule l from infinity to a distance a from molecule k

$$\Delta F_a = kT\psi_1(1 - \Theta/T)(\beta'^3/2^{1/2}\pi^{3/2})(x^2 V_s^2/V_1) \exp(-\beta'^2 a^2/2) \tag{A-3}$$

Replacement of the polymer molecular volume xV_s by $m\bar{v}$, where m is the mass of the molecule and $\bar{v}$ its specific volume, leads at once to Eq. (54) in which the quantities J, ξ, and y are defined by Eqs. (55), (56), and (57).

REFERENCES

1. G. Gee, and L. R. G. Treloar, *Trans. Faraday Soc.*, **38**, 147 (1942).
2. K. H. Meyer and R. Lühdemann, *Helv. Chim. Acta*, **18**, 307 (1935);

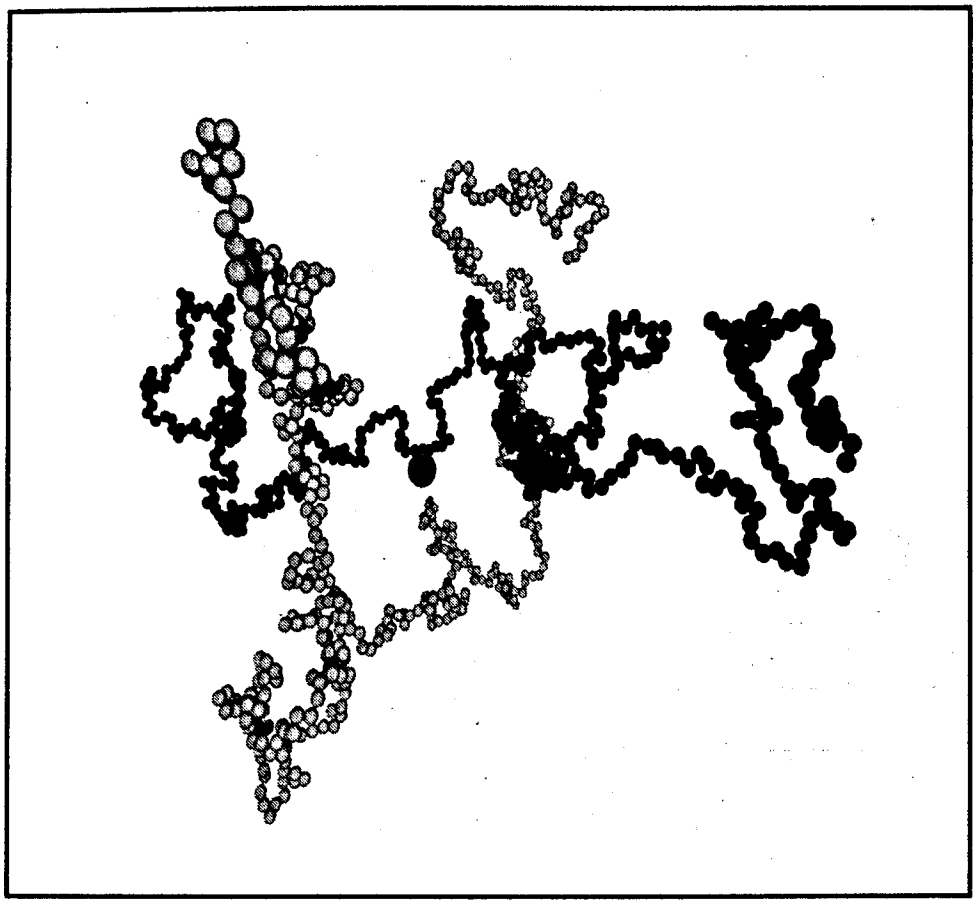

Figure 1. A snapshot from a simulation involving two self-avoiding polymers. In this configuration, the centres of mass of the two chains (denoted by the big sphere) coincide, without violation of the excluded-volume conditions. (Courtesy of Arben Jusufi.)

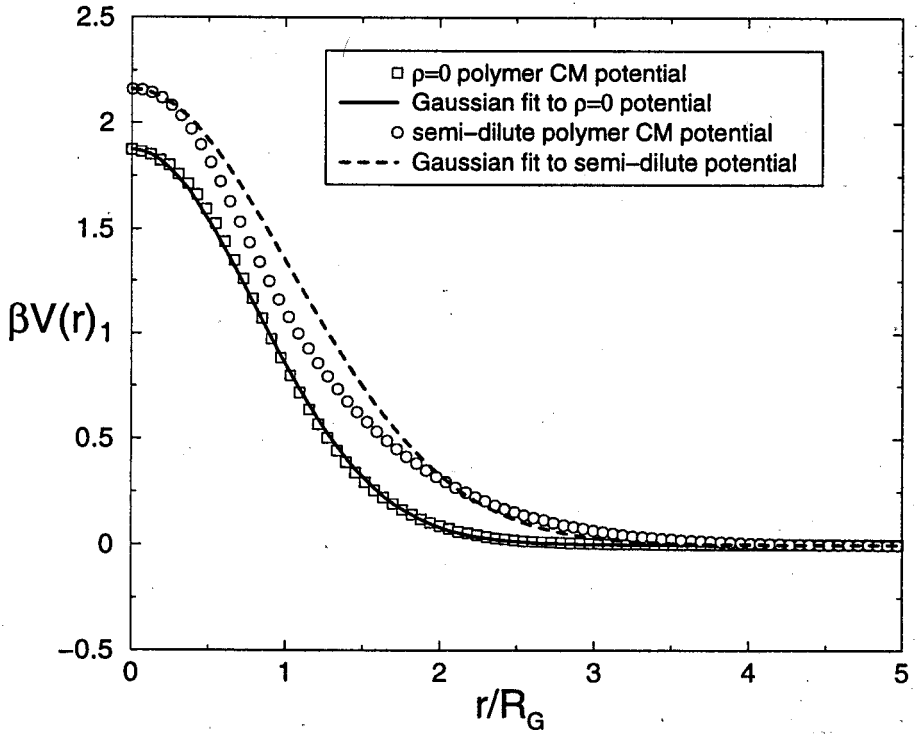

FIG. 1. Polymer center of mass potentials $\beta v(r)$ from simulations of $L = 500$ monomer SAW chains [8] are compared to a best-fit Gaussian (1), determined by fitting $\beta v(0)$ to fix $\beta\epsilon$, and $\beta\hat{v}(0)$ to fix R. The potential for two isolated coils ($\rho \to 0$) is well approximated by a Gaussian potential with $\beta\epsilon = 1.87, R = 1.13R_G$. The potential in the semi-dilute regime ($\rho \sim 4\times 3/(4\pi R_g^3)$) is approximated by a Gaussian potential with $\beta\epsilon = 2.16, R = 1.45R_G$.

Gaussian Core Model

- Basic pair interaction:

$$\varepsilon \exp\left[-(r/\sigma)^2\right], \qquad \varepsilon, \sigma > 0 .$$

- N-body potential energy (reduced units):

$$\Phi(\mathbf{r}_1 \ldots \mathbf{r}_N) = \sum_{i<j=1}^{N} \exp(-r_{ij}^{\,2}) .$$

- 3-body, 4-body, ... nonadditive interactions are not present in the Gaussian core model.

- This GCM may roughly represent the solvent-mediated interaction of polymer chains, nonionic micelles, surface-grafted colloids, ... , where pressure p represents osmotic pressure Π .

- Effect of vertical magnification:

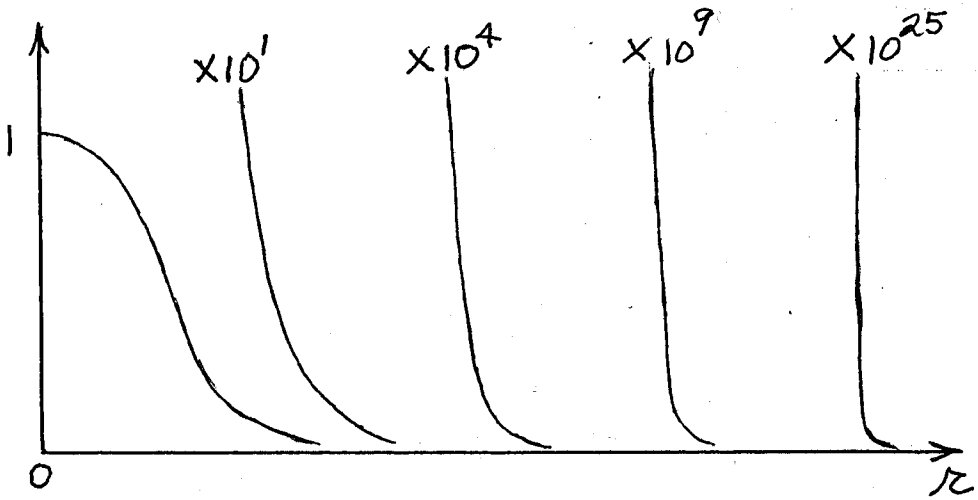

Rigid-Sphere Limit

- Pair Boltzmann factor ($\beta = 1/k_B T$):

$$b(r,\beta) = \exp\left[-\beta \exp(-r^2)\right] .$$

- $b(r,\beta)$ increases monotonically with r, attains value $1/2$ at temperature-dependent effective collision diameter:

$$r_{1/2}(\beta) = \left[\ln\left(\frac{\beta}{\ln 2}\right)\right]^{1/2} .$$

- $b(r,\beta)$ at low T approaches a unit step function:

$$b(r,\beta) \sim U\left[r - r_{1/2}(\beta)\right] .$$

The system approaches rigid-sphere kinetics and thermodynamics.

- Asymptotic curves for coexisting fluid and fcc crystal:

$$\beta_{fl}(\rho) \sim (\ln 2)\exp(0.962\rho^{-2/3}) ,$$

$$\beta_{cr}(\rho) \sim (\ln 2)\exp(1.027\rho^{-2/3}) .$$

T=0 Duality Relation

- Gaussian function is self-similar under Fourier transformation:

$$\int \exp(-r^2 + i\mathbf{k}\cdot\mathbf{r})d\mathbf{r} = \pi^{3/2}\exp(-k^2/4) \quad .$$

- Twice the lattice sum per particle (including self interaction):

$$I(\rho) = 1 + \lim_{N,V\to\infty}(2\Phi/N) \quad .$$

- Connection between reciprocal (dual) lattices:

$$\rho^{-1/2} I_{fcc}(\rho) = (\rho')^{-1/2} I_{bcc}(\rho') \quad ,$$

$$\rho\rho' = \pi^{-3} \quad .$$

- Self-dual density (equal lattice energies): $\rho = \pi^{-3/2}$.

- High density asymptotic results:

$$I_{fcc}(\rho) = \pi^{3/2}\rho\left\{1 + 8\exp\left[-\frac{3\pi^2\rho^{2/3}}{2^{4/3}}\right] + \ldots.\right\} \quad ,$$

$$I_{bcc}(\rho) = \pi^{3/2}\rho\left\{1 + 12\exp\left[-2^{1/3}\pi^2\rho^{2/3}\right] + \ldots.\right\} \quad .$$

- Upon isotropic compression, all lattice structures approach a common I value $\pi^{3/2}\rho$, with corrections of the form:

$$A\exp(-B\rho^{2/3}) \quad .$$

- High-density melting and freezing curves should have the asymptotic forms:

$$\beta_{m,f}(\rho) \sim C\exp(D\rho^{2/3}) \quad .$$

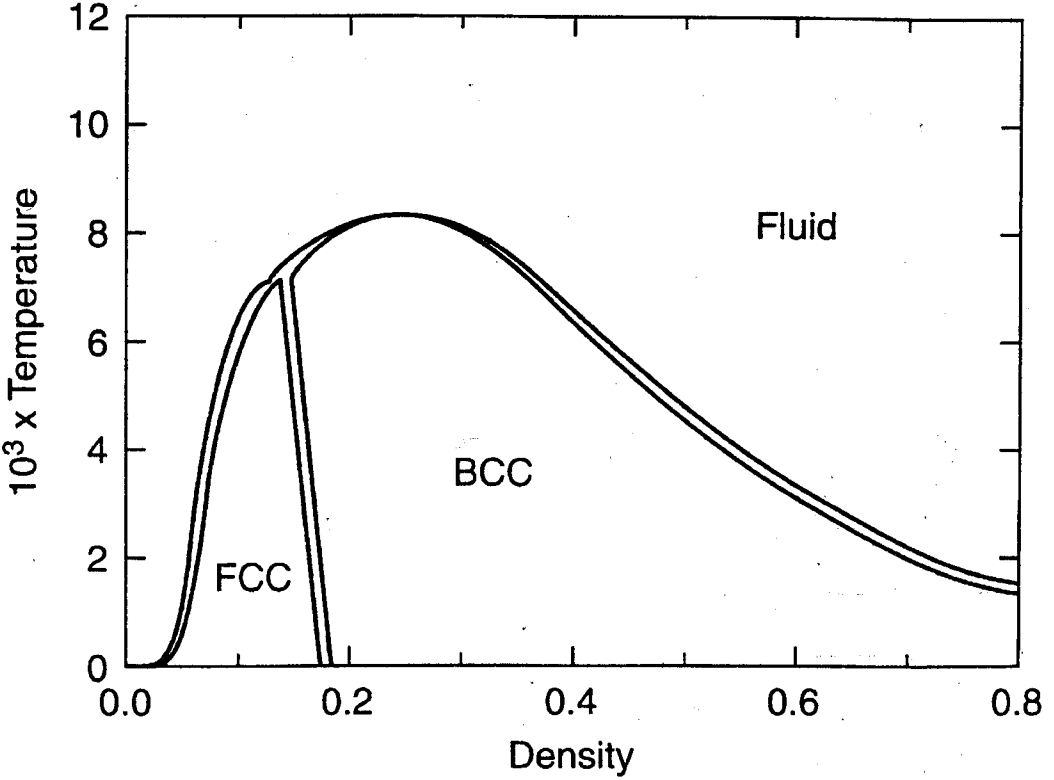
12
10
8
6
4
2
0
10^3 x Temperature
Fluid
BCC
FCC
0.0
0.2
0.4
0.6
0.8
Density

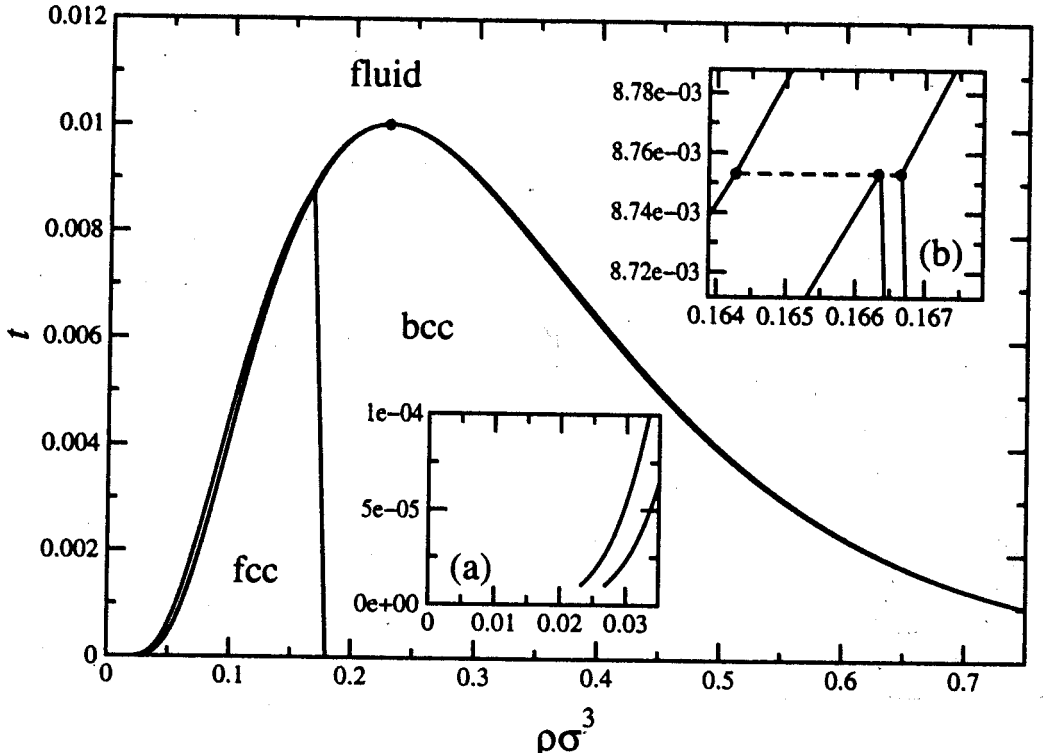

Figure 9. The phase diagram of the GCM obtained by the approach described in the text. The fcc–bcc coexistence lines are also double lines but they cannot be resolved on the scale of the figure because the fcc–bcc density gap is too small. The full dot marks the point at which the fluid–bcc coexistence curves turn around. The two insets show details of the phase diagram. (a) In the neighbourhood of zero densities and temperatures. (b) In the neighbourhood of the fluid–fcc–bcc triple temperature, with the dashed line denoting the triple line between these coexisting phases.

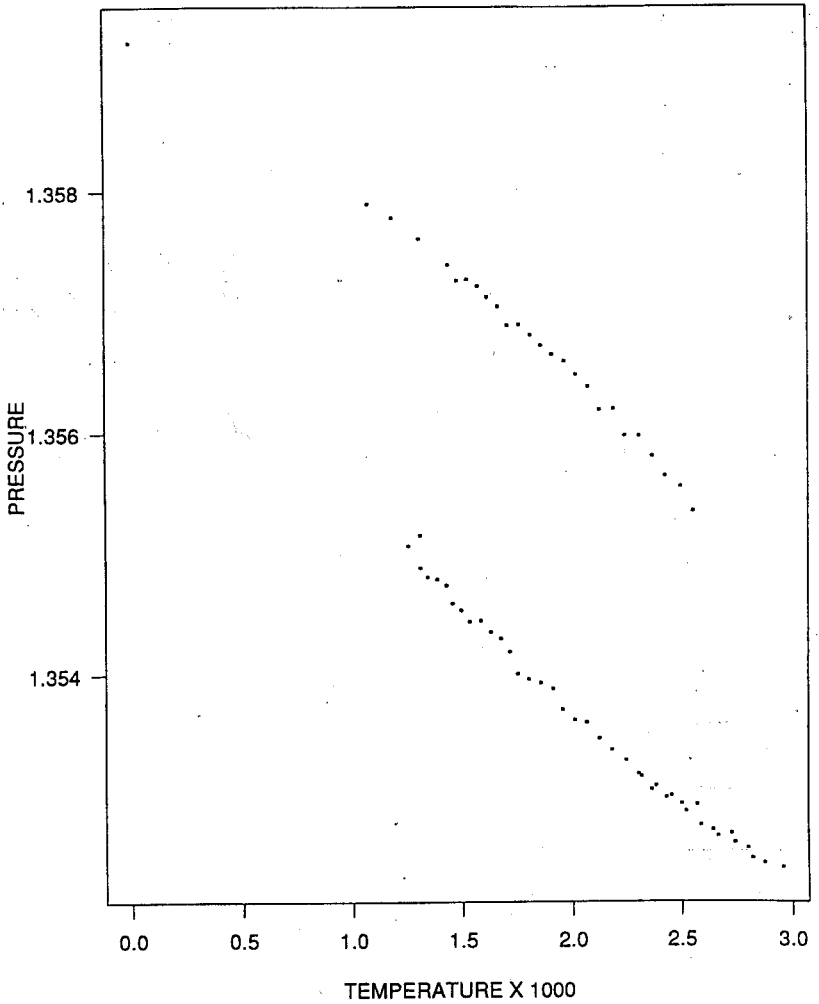

Fig. 2. Virial pressures at $\rho = 0.7$ from the molecular dynamics simulation. The upper branch refers to the BCC crystal, the lower branch to the fluid. Superheated BCC and supercooled fluid extensions are included.

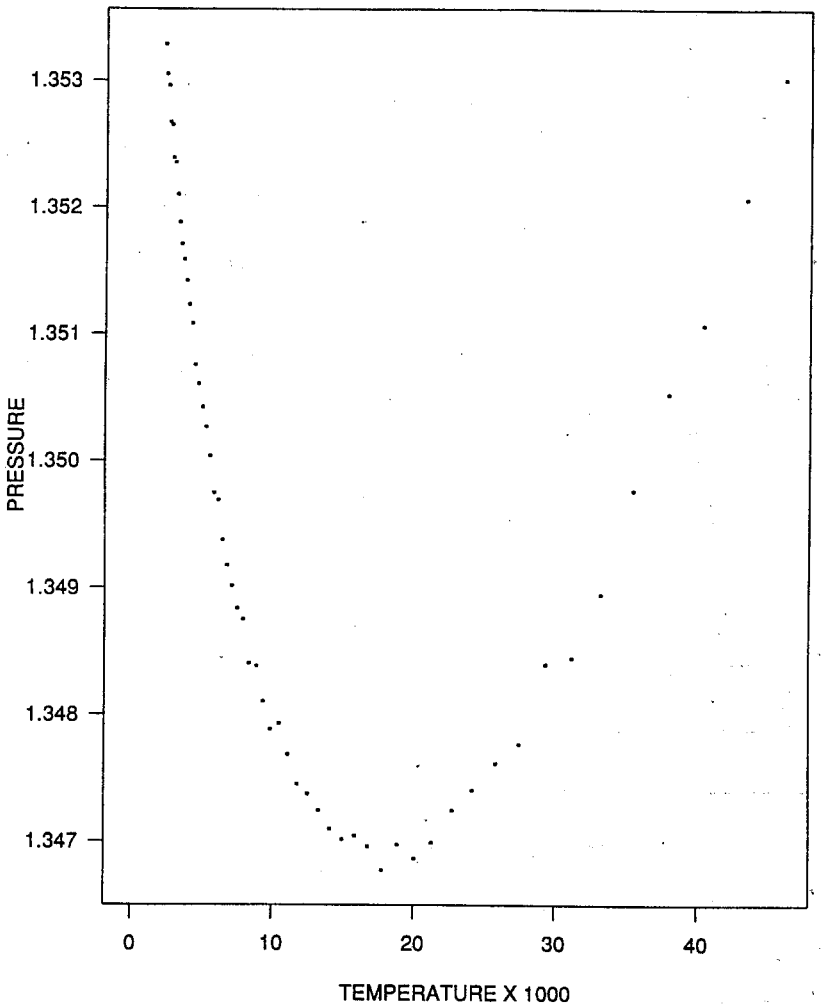

Fig. 3. Fluid-phase virial pressures for the GCM at $\rho = 0.7$ over an extended temperature range, showing a minimum.

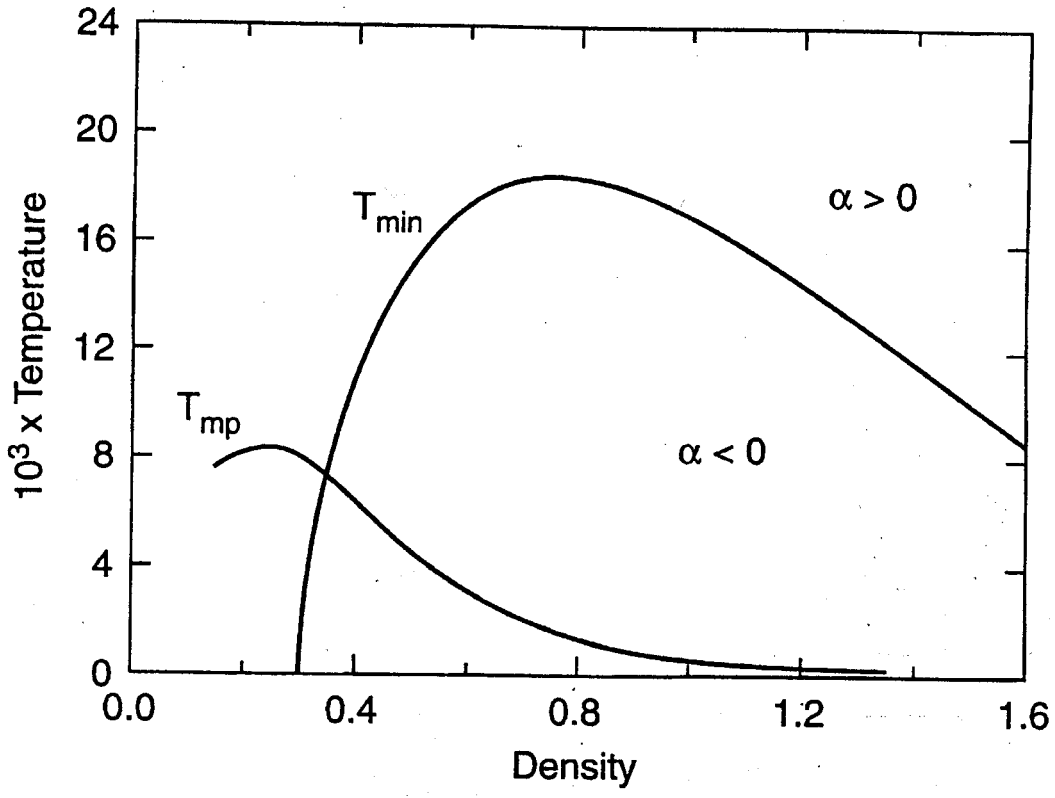

Estimated region of negative thermal expansion ($\alpha < 0$) for the classical GCM.

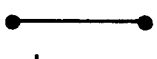

$\frac{1}{2}\pi^{D/2}$

$\frac{1}{4}(\pi/2)^{D/2}$

$\frac{1}{12}(\pi/3)^{D/2}$

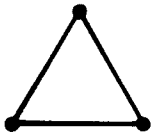

$\frac{1}{6}(\pi^2/3)^{D/2}$

$\frac{1}{48}(\pi/4)^{D/2}$

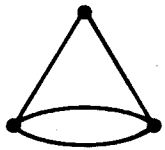

$\frac{1}{4}(\pi^2/5)^{D/2}$

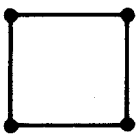

$\frac{1}{8}(\pi^3/4)^{D/2}$

FIG. 1. Low-order irreducible clusters. Under the graph of each cluster species G is given the value of $I(G)$ [Eq. (2.17)], the corresponding contribution to $\beta f(\beta)$.

TABLE I. High-temperature series coefficients for the Gaussian core model excess free energy.

n,j	Cluster species	$b_{nj}(D)$
1,2	1	$\frac{1}{2}$
2,2	1	$\frac{1}{4}(2^{-D/2})$
3,2	1	$\frac{1}{12}(3^{-D/2})$
3,3	1	$\frac{1}{6}(3^{-D/2})$
4,2	1	$\frac{1}{48}(4^{-D/2})$
4,3	1	$\frac{1}{4}(5^{-D/2})$
4,4	1	$\frac{1}{8}(4^{-D/2})$
5,2	1	$\frac{1}{240}(5^{-D/2})$
5,3	2	$\frac{1}{12}(7^{-D/2})+\frac{1}{8}(8^{-D/2})$
5,4	2	$\frac{1}{4}(7^{-D/2})+\frac{1}{4}(8^{-D/2})$
5,5	1	$\frac{1}{10}(5^{-D/2})$
6,2	1	$\frac{1}{1440}(6^{-D/2})$
6,3	3	$\frac{1}{48}(9^{-D/2})+\frac{1}{12}(11^{-D/2})+\frac{1}{48}(12^{-D/2})$
6,4	6	$\frac{1}{12}(10^{-D/2})+\frac{5}{16}(12^{-D/2})+\frac{1}{2}(13^{-D/2})+\frac{1}{24}(16^{-D/2})$
6,5	3	$\frac{1}{4}(9^{-D/2})+\frac{1}{2}(11^{-D/2})+\frac{1}{12}(12^{-D/2})$
6,6	1	$\frac{1}{12}(6^{-D/2})$
7,2	1	$\frac{1}{10\,080}(7^{-D/2})$
7,3	4	$\frac{1}{240}(11^{-D/2})+\frac{1}{48}(14^{-D/2})+\frac{1}{72}(15^{-D/2})+\frac{1}{48}(16^{-D/2})$
7,4	11	$\frac{1}{48}(13^{-D/2})+\frac{1}{24}(16^{-D/2})+\frac{1}{8}(17^{-D/2})+\frac{1}{6}(18^{-D/2})+\frac{1}{4}(19^{-D/2})+\frac{3}{16}(20^{-D/2})+\frac{1}{4}(21^{-D/2})+\frac{1}{8}(24^{-D/2})$
7,5	11	$\frac{1}{12}(13^{-D/2})+\frac{1}{4}(16^{-D/2})+\frac{1}{4}(17^{-D/2})+\frac{1}{2}(18^{-D/2})+\frac{3}{4}(19^{-D/2})+\frac{1}{3}(20^{-D/2})+\frac{1}{2}(21^{-D/2})+\frac{1}{4}(24^{-D/2})$
7,6	4	$\frac{1}{4}(11^{-D/2})+\frac{1}{2}(14^{-D/2})+\frac{1}{4}(15^{-D/2})+\frac{1}{4}(16^{-D/2})$
7,7	1	$\frac{1}{14}(7^{-D/2})$
8,2	1	$\frac{1}{80\,640}(8^{-D/2})$
8,3	5	$\frac{1}{1440}(13^{-D/2})+\frac{1}{240}(17^{-D/2})+\frac{1}{144}(19^{-D/2})+\frac{1}{192}(20^{-D/2})+\frac{1}{144}(21^{-D/2})$
8,4	22	$\frac{1}{240}(16^{-D/2})+\frac{1}{96}(20^{-D/2})+\frac{1}{32}(22^{-D/2})+\frac{1}{24}(23^{-D/2})+\frac{1}{48}(24^{-D/2})+\frac{1}{12}(25^{-D/2})+\frac{1}{12}(26^{-D/2})+\frac{1}{12}(27^{-D/2})$ $+\frac{1}{8}(28^{-D/2})+\frac{1}{6}(29^{-D/2})+\frac{1}{8}(30^{-D/2})+\frac{67}{384}(32^{-D/2})+\frac{1}{8}(35^{-D/2})+\frac{1}{32}(36^{-D/2})$
8,5	33	$\frac{1}{48}(17^{-D/2})+\frac{1}{4}(23^{-D/2})+\frac{1}{6}(25^{-D/2})+\frac{1}{2}(27^{-D/2})+\frac{3}{8}(28^{-D/2})+\frac{3}{8}(29^{-D/2})+\frac{5}{4}(31^{-D/2})+\frac{11}{16}(32^{-D/2})$ $+\frac{1}{2}(33^{-D/2})+34^{-D/2}+\frac{1}{8}(36^{-D/2})+\frac{1}{2}(37^{-D/2})+\frac{1}{2}(40^{-D/2})+\frac{1}{8}(45^{-D/2})$
8,6	23	$\frac{1}{12}(16^{-D/2})+\frac{5}{16}(20^{-D/2})+\frac{1}{4}(22^{-D/2})+\frac{1}{2}(23^{-D/2})+\frac{1}{8}(24^{-D/2})+25^{-D/2}+\frac{3}{4}(26^{-D/2})+\frac{1}{2}(27^{-D/2})$ $+\frac{5}{8}(28^{-D/2})+29^{-D/2}+\frac{3}{4}(30^{-D/2})+\frac{37}{48}(32^{-D/2})+\frac{1}{2}(35^{-D/2})+\frac{1}{8}(36^{-D/2})$
8,7	5	$\frac{1}{4}(13^{-D/2})+\frac{1}{2}(17^{-D/2})+\frac{1}{2}(19^{-D/2})+\frac{1}{4}(20^{-D/2})+\frac{1}{4}(21^{-D/2})$
8,8	1	$\frac{1}{16}(8^{-D/2})$

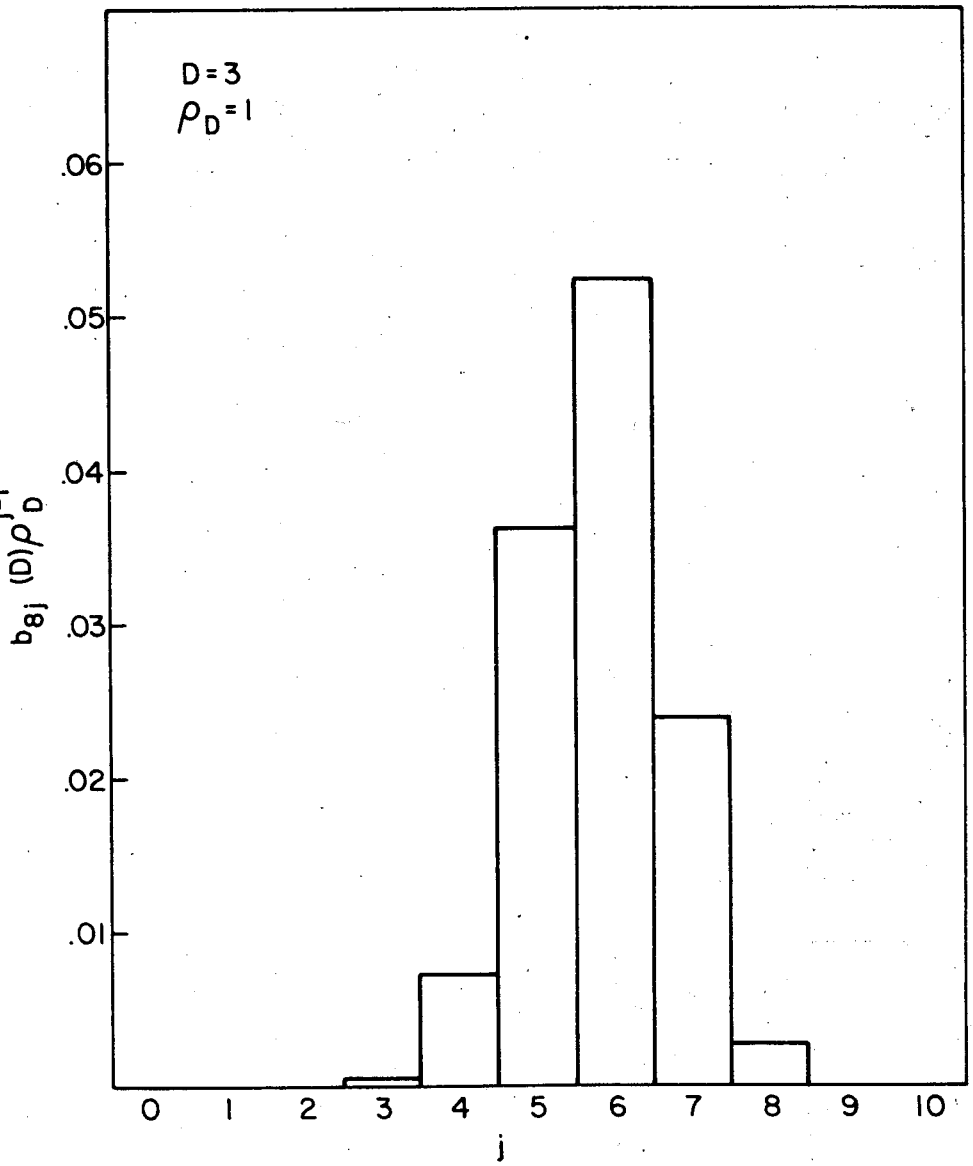

FIG. 3. Eighth-order cluster contributions $b_{8j}(D)\rho_D^{j-1}$ plotted vs j, the number of vertices. For the case shown $D = 3$ and $\rho_D = 1$.

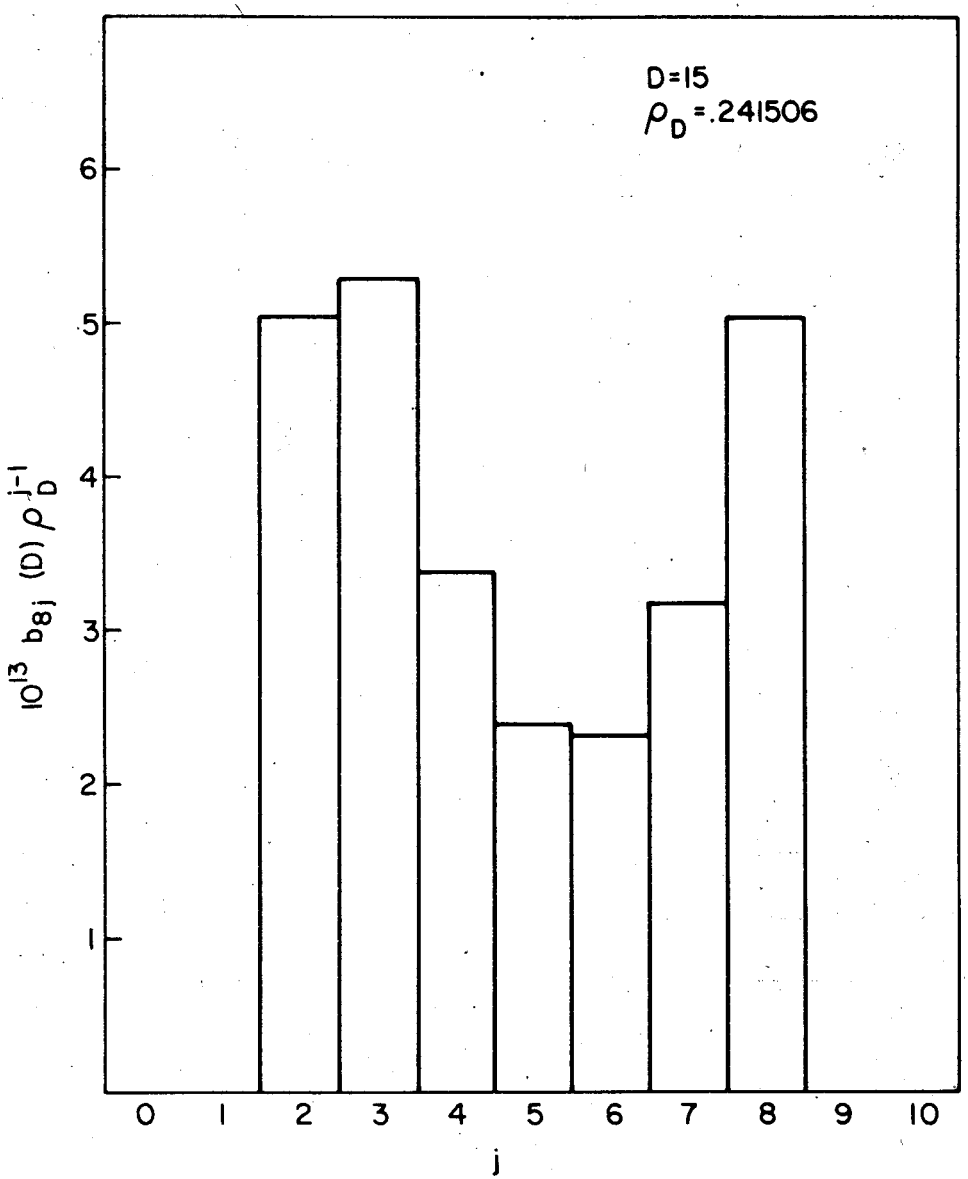

FIG. 4. Eighth-order cluster contributions vs j, for $D = 15$, $\rho_D = 0.241506$.

Compression and Gaussian Smoothing

- Change density from ρ to $(1+\varepsilon)^D \rho$.

- Behavior of Φ under uniform contraction is equivalent to a convolution with a Gaussian kernel:

$$\Phi[\mathbf{R}/(1+\varepsilon)] = (1+\varepsilon)^D \left[\pi^{1/2}(\varepsilon+\varepsilon^2/2)\right]^{-DN} \times \int \exp\left[-\frac{(\mathbf{R}-\mathbf{R}')^2}{(\varepsilon+\varepsilon^2/2)}\right] \Phi(\mathbf{R}') d^{DN}\mathbf{R}' \ .$$

- Gaussian convolution smooths small-scale variations, leaves large-scale variations, *i.e.* tends to reduce the number of local minima on Φ hypersurface.

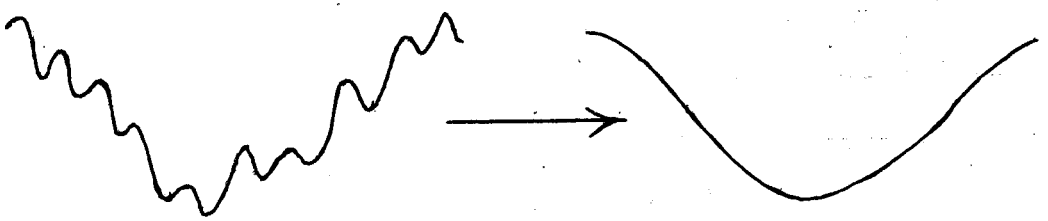

- As $\varepsilon \to \infty$, only bcc crystal minima survive.

- System has no amorphous solids ("glasses") at high density.

- Melting at high density becomes an intrabasin phenomenon.

Collective Coordinate Representation

- For N particles in rectangular volume $\Omega = L_x L_y L_z$, collective density variables are defined by:

$$\rho(\mathbf{k}) = \sum_{j=1}^{N} \exp(i\mathbf{k}\cdot\mathbf{r}_j) \ ,$$

$$\mathbf{k} = (2\pi n_x / L_x,\ 2\pi n_y / L_y,\ 2\pi n_z / L_z) \ .$$

- Alternative forms of system potential energy:

$$\Phi(\mathbf{r}_1 \ldots \mathbf{r}_N) = \sum_{i<j} v(r_{ij})$$

$$= (2\Omega)^{-1} \sum_{\mathbf{k}} V(\mathbf{k})[\rho(\mathbf{k})\rho(-\mathbf{k}) - N] \ ,$$

where: $V(\mathbf{k}) = \int_{\Omega} \exp(i\mathbf{k}\cdot\mathbf{r}) v(r) d\mathbf{r}$.

- Structure function:

$$S(k) = \langle \rho(\mathbf{k})\rho(-\mathbf{k}) \rangle$$

$$= 1 + \rho \int \exp(i\mathbf{k}\cdot\mathbf{r}) \left[g^{(2)}(r) - 1 \right] d\mathbf{r} \ .$$

- For the GCM: $V(\mathbf{k}) = \pi^{3/2} \exp(-k^2 / 4)$.

- At high density the $\mathbf{k}$'s are sparse, so $V(\mathbf{k})$ can force the $\rho(\mathbf{k})$ near the origin to their minimum value 0. If the temperature is low, this produces a sharp cutoff at

$$k_{1/2}(\beta) = 2 \left[\ln \left(\frac{\pi^{3/2} \beta}{\ln 2} \right) \right]^{1/2} \ .$$

- Structure function becomes isomorphous with low-ρ pair correlation function.

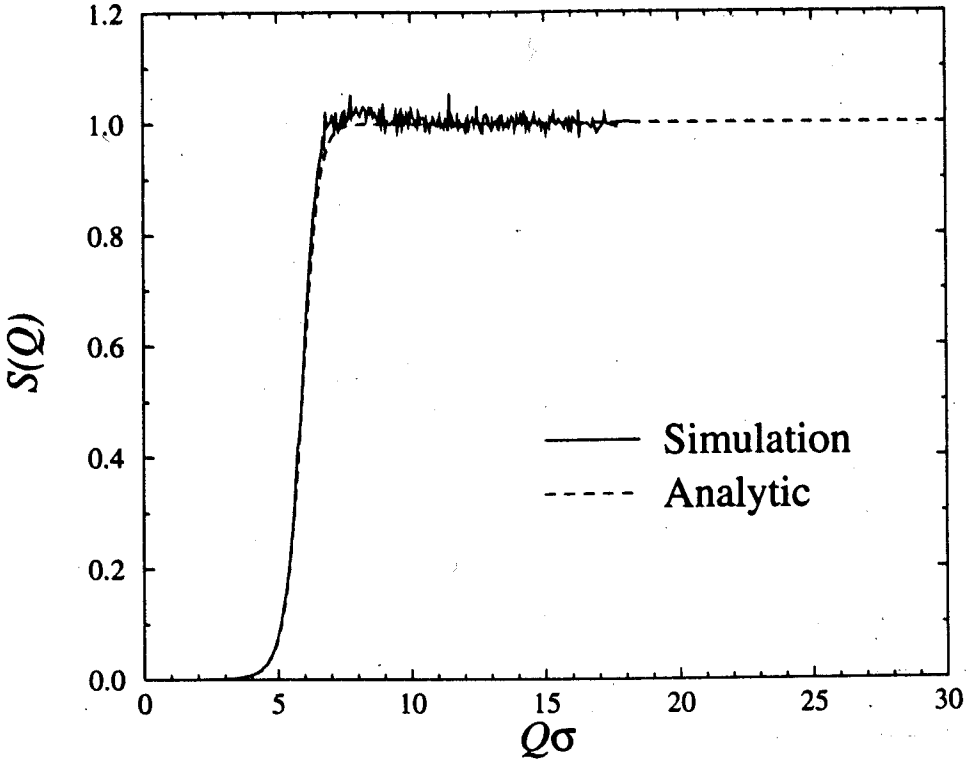

Figure 8. The structure factor $S(Q)$ of the GCM at $t = 0.01$ and $\eta = 6.00$ as obtained from simulation (solid line) and as given by the analytical expression, equation (24) (dashed line).

TABLE III. Coexistence parameters for $T=0$ structural transition.

	F.c.c.		B.c.c.
ρ	0.17941		0.17977
Φ/N	0.115465107		0.116073318
p		0.05529	
$\Delta\rho$		0.00036	
$\Delta(\Phi/N)$		0.000608211	

Challenges to Synthetic Chemistry and to Theoretical Modeling

Identify backbone modification, side-group inclusion, and solvent composition for which:

(a) the GCM in its simplest version is an accurate description; or if that is not possible, then

(b) produce materials/models for which an extended version of the GCM has 3-body, 4-body, … nonadditive interactions that are Gaussian functions of the chain-centroid coordinates; or if that is not possible, then

(c) produce materials/models for which the interactions are other functions beside simple Gaussians that are self-similar under Fourier transformation.